

UNCLASSIFIED

AD NUMBER: AD1042986

LIMITATION CHANGES

TO:

Approved for public release; distribution is unlimited.

FROM:

Distribution authorized to Department of Defense and U.S. DoD contractors only; Critical Technology; 03/01/2017; Other requests shall be referred to Environmental Security Technology Certification Program, Alexandria, VA, 22350.

AUTHORITY

SERDP memo dtd 10 Jan 2018

THIS PAGE IS UNCLASSIFIED



January 10<sup>th</sup>, 2018

Defense Technical Information Center  
DTIC-CQ  
8725 John J. Kingman Road  
Fort Belvoir, VA 22060

To whom it may concern:

The distribution statement initially submitted with AD1042986, entitled Underwater Advanced Time Domain Electromagnetic System (MR-201313), has been appealed successfully, and should be changed from D to A.

Attached to this message is the DD1910 form denoting its status as being cleared for public distribution.

The Defense Office of Prepublication and Security Review (DOPSR) has been contacted, and concurs with the judgement of this office and its subject matter experts. If you have further questions for DOPSR please contact Mr. Donald Kluzik at 703-614-4931, email: [donald.e.kluzik.civ@mail.mil](mailto:donald.e.kluzik.civ@mail.mil), citing case # 17-S-2228.

Sincerely,

Herbert Nelson, Ph.D.  
Acting Executive Director  
Strategic Environmental Research  
and Development Program  
Environmental Security Technology  
Certification Program

# DEMONSTRATION REPORT

Underwater Advanced Time-Domain Electromagnetic System

ESTCP Project MR-201313

MARCH 2017

Mr. Steve Saville  
CH2M

Distribution Statement A:  
Approved for Public Release.

~~Distribution Statement D: Distribution  
authorized to the Department of Defense  
and U.S. DoD contractors only.~~



*Page Intentionally Left Blank*

This report was prepared under contract to the Department of Defense Environmental Security Technology Certification Program (ESTCP). The publication of this report does not indicate endorsement by the Department of Defense, nor should the contents be construed as reflecting the official policy or position of the Department of Defense. Reference herein to any specific commercial product, process, or service by trade name, trademark, manufacturer, or otherwise, does not necessarily constitute or imply its endorsement, recommendation, or favoring by the Department of Defense.

*Page Intentionally Left Blank*

| REPORT DOCUMENTATION PAGE   |             |  |                               | Form Approved<br>OMB No. 0704-0188                         |  |
|---|-------------|--|-------------------------------|--|--|
| Public reporting burden for this collection of information is estimated to average 1 hour per response, including the time for reviewing instructions, searching existing data sources, gathering and maintaining the data needed, and completing and reviewing this collection of information. Send comments regarding this burden estimate or any other aspect of this collection of information, including suggestions for reducing this burden to Department of Defense, Washington Headquarters Services, Directorate for Information Operations and Reports (0704-0188), 1215 Jefferson Davis Highway, Suite 1204, Arlington, VA 22202-4302. Respondents should be aware that notwithstanding any other provision of law, no person shall be subject to any penalty for failing to comply with a collection of information if it does not display a currently valid OMB control number. <b>PLEASE DO NOT RETURN YOUR FORM TO THE ABOVE ADDRESS.</b> |             |  |                               |  |  |
| 1. REPORT DATE (DD-MM-YYYY)<br>03-03-2017   |             | 2. REPORT TYPE<br>Demonstration Report |                               | 3. DATES COVERED (From - To)                               |  |
| 4. TITLE AND SUBTITLE<br><br>Underwater Advanced Time-Domain Electromagnetic System   |             |  |                               | 5a. CONTRACT NUMBER  |  |
|   |             |  |                               | 5b. GRANT NUMBER   |  |
|   |             |  |                               | 5c. PROGRAM ELEMENT NUMBER                                 |  |
| 6. AUTHOR(S)<br><br>Steve Saville   |             |  |                               | 5d. PROJECT NUMBER   |  |
|   |             |  |                               | 5e. TASK NUMBER  |  |
|   |             |  |                               | 5f. WORK UNIT NUMBER                                       |  |
| 7. PERFORMING ORGANIZATION NAME(S) AND ADDRESS(ES)<br><br>CH2M<br>2411 Dulles Corner Park, Suite 500<br>Herndon, VA 20171   |             |  |                               | 8. PERFORMING ORGANIZATION REPORT<br>NUMBER                |  |
| 9. SPONSORING / MONITORING AGENCY NAME(S) AND ADDRESS(ES)<br>Environmental Security Technology Certification Program<br>4800 Mark Center Drive, Suite 17D03<br>Alexandria, VA 22350   |             |  |                               | 10. SPONSOR/MONITOR'S ACRONYM(S)<br><br>ESTCP              |  |
|   |             |  |                               | 11. SPONSOR/MONITOR'S REPORT<br>NUMBER(S)<br><br>MR-201313 |  |
| 12. DISTRIBUTION / AVAILABILITY STATEMENT<br><br>Distribution A.  |             |  |                               |  |  |
| 13. SUPPLEMENTARY NOTES   |             |  |                               |  |  |
| 14. ABSTRACT<br>The overall objective of the project is to design, build and demonstrate an underwater advanced time-domain electromagnetic (TEM) system for cued classification of munitions in the underwater environment. The phased approach consists of initial design and modeling (Phase 1 –completed), engineering design and construction (Phase 2 –completed), underwater evaluation of the system (Phase 3 – described in this document), and an optional Phase 4 demonstration of the system at a field site.   |             |  |                               |  |  |
| 15. SUBJECT TERMS<br>Underwater, time-domain, electromagnetic system, freshwater, munitions   |             |  |                               |  |  |
| 16. SECURITY CLASSIFICATION OF:   |             |  | 17. LIMITATION<br>OF ABSTRACT | 18. NUMBER<br>OF PAGES<br><br>36                           | 19a. NAME OF RESPONSIBLE PERSON<br>Steve Saville             |
| a. REPORT<br>Demonstration<br>Report  | b. ABSTRACT | c. THIS PAGE                           |                               |  | 19b. TELEPHONE NUMBER (include area<br>code)<br>202-596-1199 |

*Page Intentionally Left Blank*



# Contents

| Section   | Page     |
|---|----------|
| <b>System Performance Report</b>  | <b>1</b> |
| Introduction  | 1        |
| Project Description   | 1        |
| Technology  | 1        |
| Facility and Support  | 3        |
| System Setup and Testing  | 5        |
| Test Strip  | 5        |
| Conductivity Measurements   | 7        |
| System Issue  | 8        |
| Sensor Function Test  | 8        |
| In-air and In-water Response Test   | 9        |
| Background Response Test  | 11       |
| Board Tests   | 15       |
| Buried Target Measurements  | 17       |
| Performance Objectives  | 20       |
| Objective: System is sufficiently waterproofed  | 20       |
| Objective: Calibration method can be used both topside and underwater   | 20       |
| Objective: Classification can be achieved if item is anywhere within physical footprint of system   | 20       |
| Objective: Sensor response repeatability (cued surveys)   | 21       |
| Objective: Sensor can be deployed using winch and donut approach  | 21       |
| Objective: Sensor can be sufficiently maneuvered in underwater environment by divers such that the divers' safety is not compromised  | 21       |
| Objective: Sensor can be sufficiently maneuvered in underwater environment by divers such that the system can be placed satisfactorily on the desired cue location to collect classification data | 22       |
| Objective: Inversion results support classification   | 23       |
| Objective: Inversion result provides correct position   | 23       |
| Objective: Classification is valid  | 23       |
| Summary and Path Forward  | 27       |

## Figures

|    |  |
|----|--|
| 1  | Underwater Advanced Time-Domain Electromagnetic System   |
| 2  | Photograph of Underwater Advanced Time-Domain Electromagnetic System   |
| 3  | Transmitter and receiver locations and nomenclature  |
| 4  | NSWCPCD's freshwater pond facility   |
| 5  | Crane provided by NSWCPCD for transfer of system from land into water  |
| 6  | Inner-tube shallow water lift system and dive team for maneuvering system from within the water                      |
| 7  | As-built diagram of test strip   |
| 8  | Photographs of test objects prior to burial  |
| 9  | Aluminum ball over TxA/RxB during sensor function test   |
| 10 | Sensor Function Test performance   |
| 11 | In-air (on deck) and in-water response measurements made with aluminum ball supported above the array on a PVC stand |

**Figures (Cont.)**

- 12 Average background response for monostatic TxC/RxG pair, Z-axis, at several locations
- 13 Average background response for monostatic TxC/RxG pair at background location B1
- 14 Median measurement-to-measurement background variability for various transmit/receive combinations
- 15 Background variability for various transmit/receive combinations for measurements spread out in time and/or space
- 16 Left: Test board mounted above array, with medium and large ISO targets Right: Drawing showing test board dimensions and location relative to array
- 17 Board test results for the 6½ cm x 20 cm steel ellipsoid (top row), the large ISO (middle row) and the medium ISO (bottom row)
- 18 Buried target fit locations for ISOs and inert munitions
- 19 Graph showing the relationship of the distance from the center of the array of each object during measurement to the library match
- 20 Overlay of monostatic Z-axis responses (blue) and Z-axis responses with outer (H) transmitter (red) for no diver and two measurements with a diver standing by the battery box

**Tables**

- 1 Pond water measurements
- 2 Sensor white noise levels ( $\mu\text{T}/\text{As}$ )
- 3 Dipole fit parameters for targets on test board
- 4 Cued target fit parameters
- 5 Performance Objectives and Results

# Acknowledgments

The CH2M project team for the underwater testing at the Naval Surface Warfare Center Panama City Division (NSWC-PCD) included the following Key Personnel who all played an integral role.

| Name          | Affiliation | Responsibilities            |
|---------------|-------------|-----------------------------|
| Tamir Klaff   | CH2M        | Principal Investigator      |
| Kelsey Dubois | Geometrics  | Project Engineer            |
| Nick Odum     | Geometrics  | Application Geophysicist    |
| John Nichols  | Geometrics  | Project Engineer            |
| Tom Bell      | Leidos      | Data Analysis and Reporting |
| Bruce Barrow  | Acorn SI    | Data Analysis and Reporting |
| Ray Lim       | NSWC PCD    | Site Coordinator            |

CH2M would also like to thank NSWC-PCD staff Lisa Arrieta and Russ Malcolm and the dive support team, led by Steve Lowe, for their fantastic support during the field operation.

# System Performance Report

---

## Introduction

This document has been prepared under Environmental Security Technology Certification Program (ESTCP) Project MR-201313, titled Underwater Advanced Time-Domain Electromagnetic System, to present results of the system evaluation performed by CH2M HILL, Inc. (CH2M) at the Naval Surface Warfare Center (NSWC) Panama City Division's (PCD's) freshwater pond facility in October 2016. The intent of the testing was to perform a field evaluation of the system designed and constructed in the initial phases of the project.

## Project Description

The overall objective of the project is to design, build and demonstrate an underwater advanced time-domain electromagnetic (TEM) system for cued classification of munitions in the underwater environment. The phased approach consists of initial design and modeling (Phase 1 –completed), engineering design and construction (Phase 2 –completed), underwater evaluation of the system (Phase 3 – described in this document), and an optional Phase 4 demonstration of the system at a field site.

## Technology

The system designed and constructed under this project has been described in detail in prior documents, titled *Modeling for Underwater Advanced Time-Domain Electromagnetic System* (June, 2014), *Underwater Advanced Time-Domain Electromagnetic System Design* (July, 2015), and in the *Underwater Advanced Time-Domain Electromagnetic System Evaluation Plan* (October, 2016). A diagram of the system, as tested, is provided as **Figure 1**. A photograph of the system is provided as **Figure 2**.

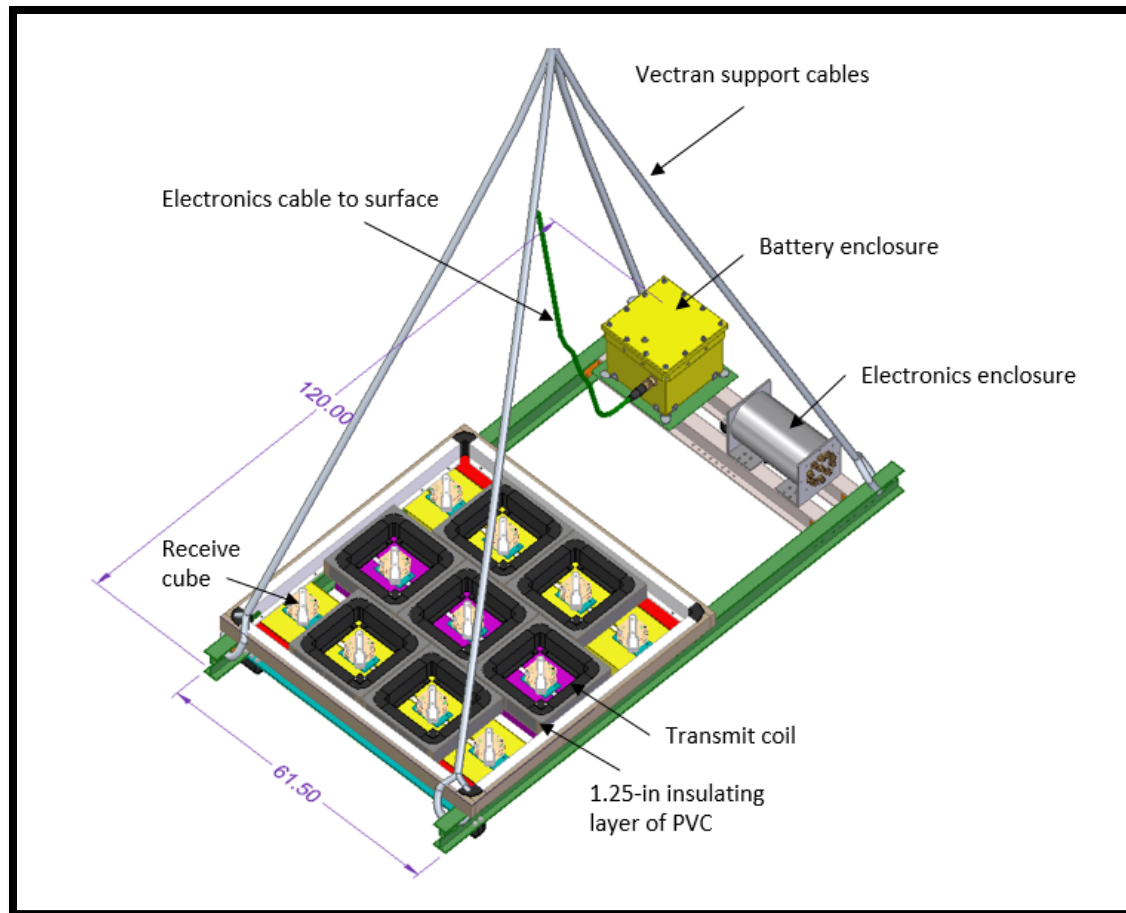


**Figure 1. Underwater Advanced Time-Domain Electromagnetic System. Measurements are in inches.**



**Figure 2. Photograph of Underwater Advanced Time-Domain Electromagnetic System**

**Figure 3** presents a diagram identifying transmitter (Tx) and receiver (Rx) locations and nomenclature. The array consists of eleven 10 centimeter (cm) three-axis receive cubes, denoted by the cube identifier and an “r” indicating “receiver” (i.e. Ar-Kr), seven 40 cm square transmit coils, denoted by the cube identifier and a “t” indicating “transmitter” (i.e. At-Gt), and an outer 1.56 m square transmit coil (Ht). The resulting total number of data channels is 264. The raw sampling interval used for the evaluation was 0.004 ms and the recorded data were logarithmically averaged over 5% windows, resulting in 99 logarithmically spaced decay times ranging from 0.05 milliseconds (ms) to 8.124 ms. One hundred measurements were averaged for each recorded measurement.

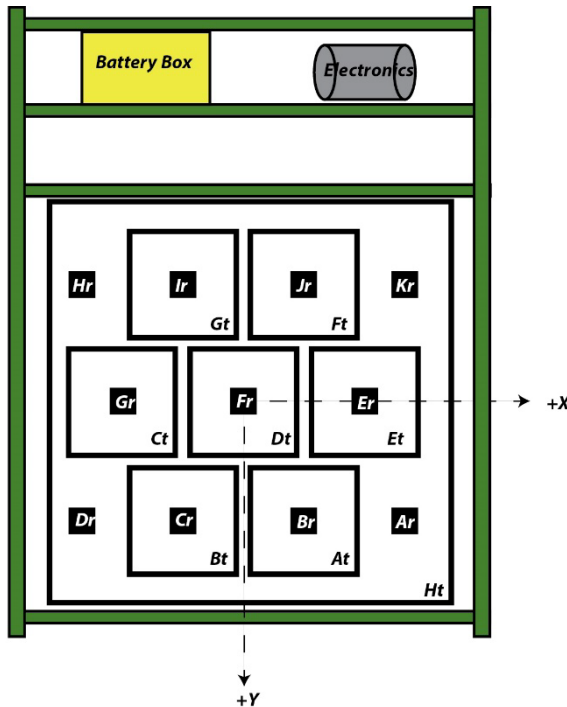


**Figure 3.** Transmitter and receiver locations and nomenclature.

## Facility and Support

Dive operations, crane support, and general logistical support were provided by NSWCPD. The NSWCPD pond, shown by **Figure 4**, is 110 meter (m) wide by 80 m long and 13.5 m deep. A 30 m by 50 m bed of sand is located in the center of the pond. The pond was “shocked” on October 5, 2016 with 1800 pounds (lbs) of Calcium Hypochlorite followed by 12 cases of flocculent on October 7, 2016; however, by October 12 when the system was first introduced into the water the visibility was limited to a few feet and there was almost no visibility at times for the divers when the test bed sediment was disturbed by their activities.

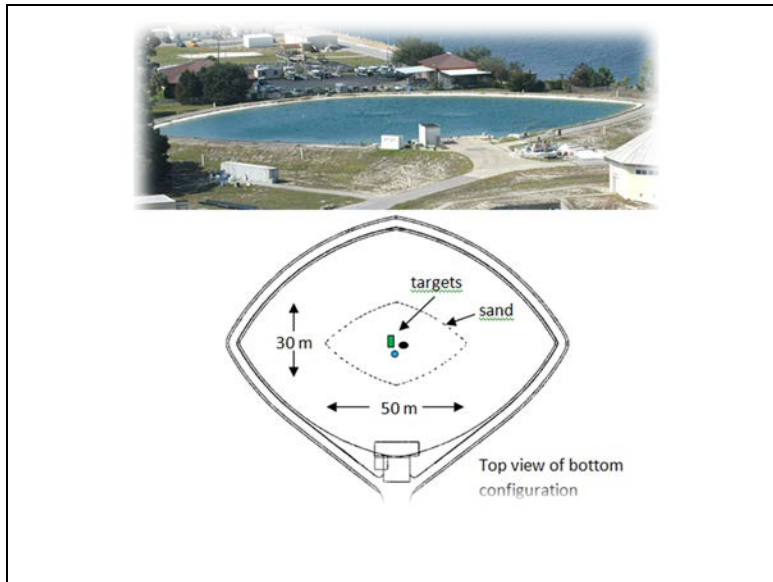


**Figure 4.** NSWPCD's freshwater pond facility.

NSWPCD provided a crane (see **Figure 5**), operator, and riggers for deployment of the system into and out of the pond, an inner-tube shallow water lift system with a 2500lb lift capacity crane (see **Figure 6**), and a team of divers to maneuver the inner-tube and the system.



**Figure 5.** Crane provided by NSWPCD for transfer of system from land into water.





Figure 6. Inner-tube shallow water lift system and dive team for maneuvering system from within the water.

## System Setup and Testing

CH2M and its subcontractors, Geometrics Inc. (Geometrics) and Leidos, mobilized to NSWPCD on October 10, 2016. System setup, initial sensor function tests, and establishment of an underwater test strip were performed on October 11, 2016. In-water tests on October 12 and 13 included background response measurements, board tests to check the accuracy of target locations and polarizabilities determined by inverting array data under controlled conditions, and buried target measurements.

### Test Strip

A test strip, shown by **Figure 7**, was established by the dive team on October 11, 2016 along the north-south centerline of the pond using a rope and markers on the rope with objects buried at the marked locations beneath the surface of the sand. Objects were spaced at approximately 10 m increments to allow for enough space in between them for the collection of background measurements. The objects buried, photographs of which are shown in **Figure 8**, approximate depths, and their placement orientations consisted of:

1. Large industry standard object (ISO) (4-inch x 12-inch steel pipe<sup>1</sup>), approximately 1-2 foot depth, long axis approximately 30 degrees from the strip centerline
2. 105-millimeter projectile, approximately 1-2 foot depth, long axis oriented parallel to the strip centerline
3. 105-millimeter High Explosive Anti-Tank (HEAT) projectile, approximately 1-2 foot depth, long axis approximately 30 degrees from the strip centerline
4. 3-inch by 12-inch aluminum rod, approximately 6 inches depth, with its long axis approximately 30 degrees from the strip centerline
5. Medium ISO (2-inch x 8-inch steel pipe<sup>2</sup>), approximately 6 inches depth, with its long axis approximately 30 degrees from the strip centerline

<sup>1</sup> <https://www.mcmaster.com/#44615k137/=155225y>

<sup>2</sup> <https://www.mcmaster.com/#44615k529/=15525a7>



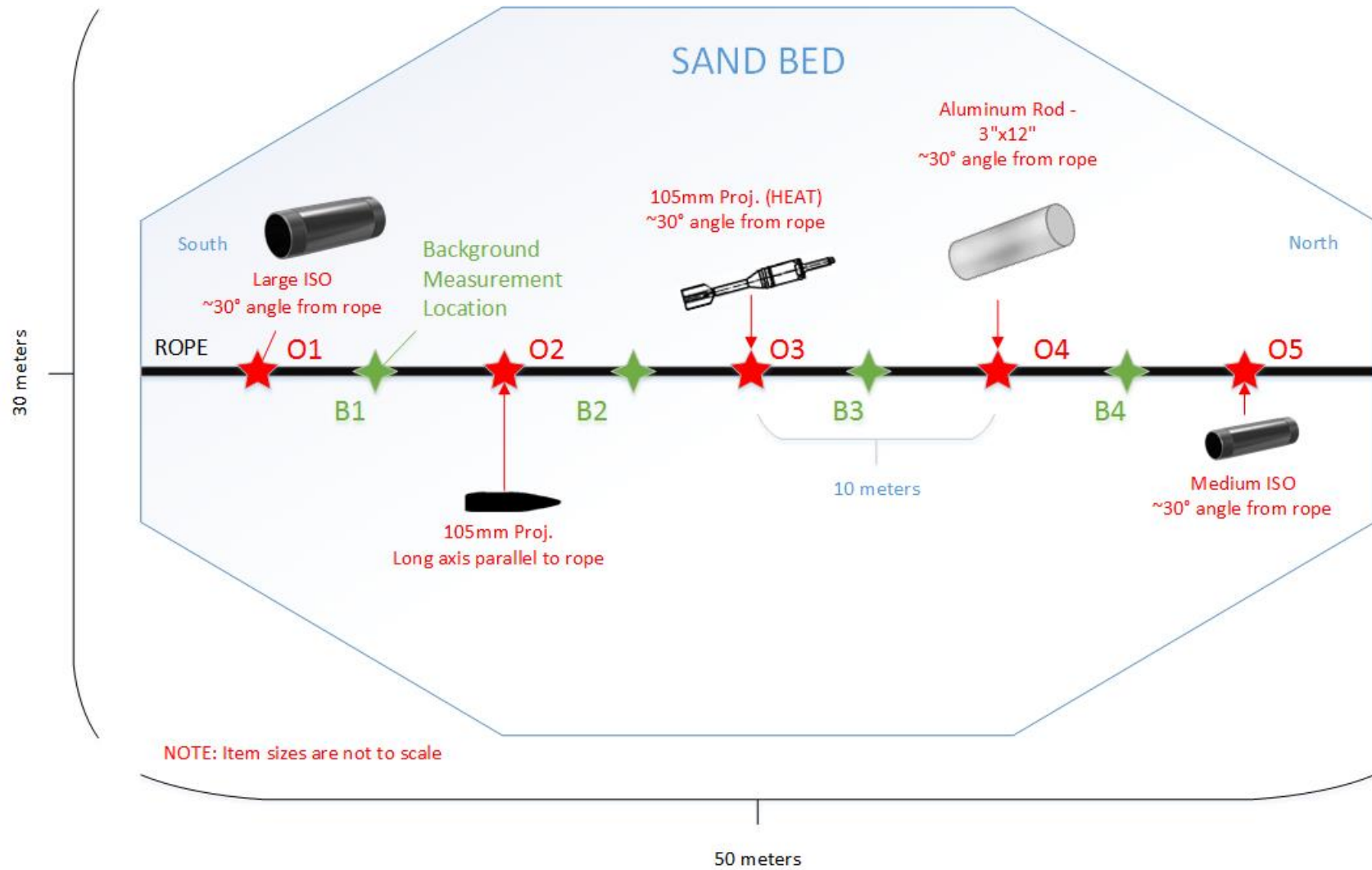


Figure 7. As-built diagram of test strip.



**Figure 8. Photographs of test objects prior to burial. (Intended burial depths and orientations relative to the centerline of the test strip were marked on the objects.)**

## Conductivity Measurements

After construction of the test strip, an Aqua Troll 200<sup>3</sup> was used to collect conductivity and other pond water parameter measurements directly above the burial locations of the objects, the results of which are shown in **Table 1**. The average values for actual conductivity and specific conductivity were 313 micro-siemens per centimeter ( $\mu\text{S}/\text{cm}$ ) and 303  $\mu\text{S}/\text{cm}$ , respectively. Typical seawater conductivity<sup>4</sup> is around 50,000  $\mu\text{S}/\text{cm}$  and conductivity in most freshwater streams<sup>5</sup> is between 50 to 1500  $\mu\text{S}/\text{cm}$ , thus the testing was performed in freshwater conditions.

<sup>3</sup> <https://in-situ.com/products/water-level-monitoring/aqua-troll-200-data-logger/>

<sup>4</sup> <http://www.lenntech.com/applications/ultrapure/conductivity/water-conductivity.htm>

<sup>5</sup> <http://fosc.org/WQData/WQParameters.htm>

Table 1. Pond water measurements

| Parameter                          | OBJECT |        |        |        |        | Average |
|------------------------------------|--------|--------|--------|--------|--------|---------|
|                                    | 1      | 2      | 3      | 4      | 5      |         |
| Temp (°C)                          | 26.7   | 26.8   | 26.7   | 26.7   | 26.8   | 26.7    |
| Pressure (PSI)                     | 16.5   | 16.7   | 16.7   | 16.5   | 16.6   | 16.6    |
| Depth (ft)                         | 38     | 38.5   | 38.6   | 38.2   | 38.2   | 38.3    |
| Actual Conductivity (μS/cm)        | 272.6  | 174.9  | 382.1  | 356.3  | 379.5  | 313.1   |
| Specific Conductivity (μS/cm)      | 263.8  | 169.2  | 370.2  | 345.4  | 367.1  | 303.1   |
| Resistivity (ohm-cm)               | 3668.7 | 5718.6 | 2617.1 | 2806.5 | 2635.1 | 3489.2  |
| Salinity (PSU)                     | 0.126  | 0.08   | 0.179  | 0.166  | 0.177  | 0.146   |
| Total Dissolved Solids (ppt)       | 0.017  | 0.11   | 0.241  | 0.224  | 0.239  | 0.166   |
| Water Density (g/cm <sup>3</sup> ) | 0.997  | 0.997  | 0.997  | 0.997  | 0.997  | 0.997   |

**NOTES**

°C = degrees Celsius

PSI = pounds per square inch

ft = feet

μS/cm = microsiemen per centimeter

PSU = practical salinity unit

ppt = parts per thousand

g/cm<sup>3</sup> = grams per cubic centimeter

## System Issue

Early in the data collection process it was determined that the signal was not being recorded properly for approximately 15% of the receiver cube channels from any particular measurement, but it was (for the most part) inconsistent which channels were affected. Troubleshooting in the field was not successful in identifying the cause of the issue, but the team determined that the data could still be used for classification. The electronics box was returned to Geometrics after completion of the pond testing and it was determined that the signal was being read in, but was extremely low and was not being recognized by the acquisition software. Further testing determined that the corrupt data were caused by incorrect delay values in the field-programmable gate array (FPGA) firmware that are affected by rising temperatures in the electronics canister, and this caused changes in the behavior of the serial lines on the analog-to-digital conversion hardware (specifically the FPGA Mezzanine Card [FMC] boards). The changes moved the converted digital signal partly out of the timing window during which the de-serialization hardware retrieves the data, resulting in mis-scaled or otherwise bad data. The host software controls the location of that hardware timing window by transmitting some FMC delays during startup and these delay values are determined empirically, during testing. Geometrics is in the process of determining the correct FMC delay values and their validity in varying thermal conditions, and developing tools to manage them during follow-up system work.

## Sensor Function Test

A sensor function test was performed on the system after setup on October 11, 2016. The function test entailed measuring the response to a standard 4-inch diameter aluminum ball positioned above each of the receivers. **Figure 9** shows the aluminum ball above the array positioned over the A transmitter and B receiver (refer to **Figure 3** for transmitter and receiver nomenclature).

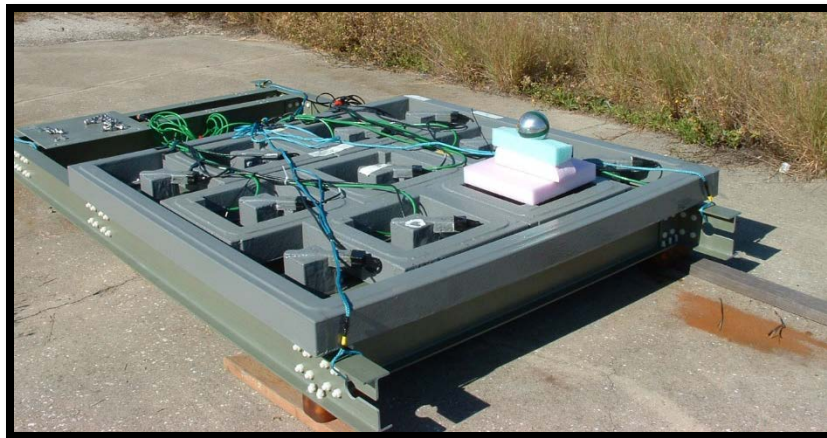


**Figure 9. Aluminum ball over TxA/RxB during sensor function test.**

Results for the sensor function test with the array on the deck (in air) on the first day are shown by **Figure 10**. Signal levels are in microTesla per Ampere-second ( $\mu\text{T}/\text{As}$ ). Plot (a) (on the left) shows Z-axis responses for all of the monostatic transmit-receive TxRx pairs (the seven co-located transmitters and receivers). Negative signals are in red, positive in blue. All of the responses should be roughly identical. The odd blue curve is for the E receiver, which malfunctioned (see System Issue section above). The remaining six curves have a total spread in amplitude of  $\pm 2.8\%$ . The middle plot (b) shows similar results for the ball over the corner receivers with the outer transmitter loop. By symmetry the responses should be identical. The observed spread was  $\pm 5.7\%$ . The plot on the right (c) shows corresponding responses for the inner sets of receivers at the front and back of the array (B, C, I and J). Again, by symmetry they should have roughly identical responses. In this case the observed spread was  $\pm 2.9\%$ . The sensor function test was not repeated with the array in the pond.

## In-air and In-water Response Test

Identical in-air and in-water response measurements were made with the aluminum ball supported above the array on a PVC stand. The data were inverted using the UX-Analyze dipole fit algorithm and target locations calculated by inverting the in-air and in-water data were within 6 millimeters (mm) of each other. As shown by **Figure 11**, there was no discernable difference between the in-air and in-water polarizabilities; they were a near perfect match to each other based on the UX-Analyze classification algorithm. The PVC mounting broke after the first set of tests and the test was not repeated.

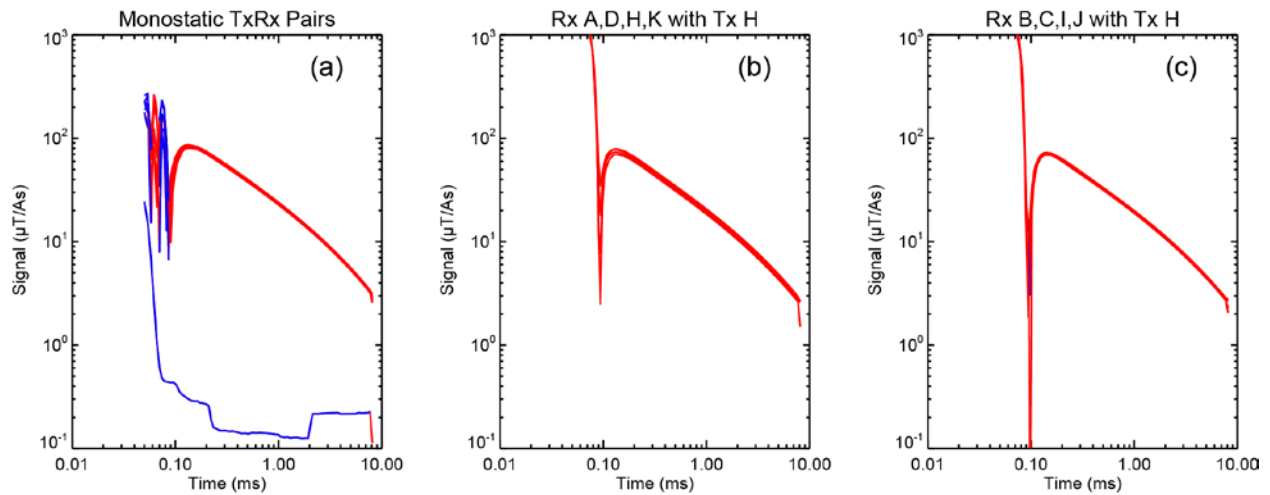


Figure 10. Sensor Function Test performance. (a) Measured Z-axis response to 4" aluminum ball for each monostatic TxRx pair. (b) Response for corner receivers with outer loop Tx. Response for inner front and back receivers with outer loop Tx.

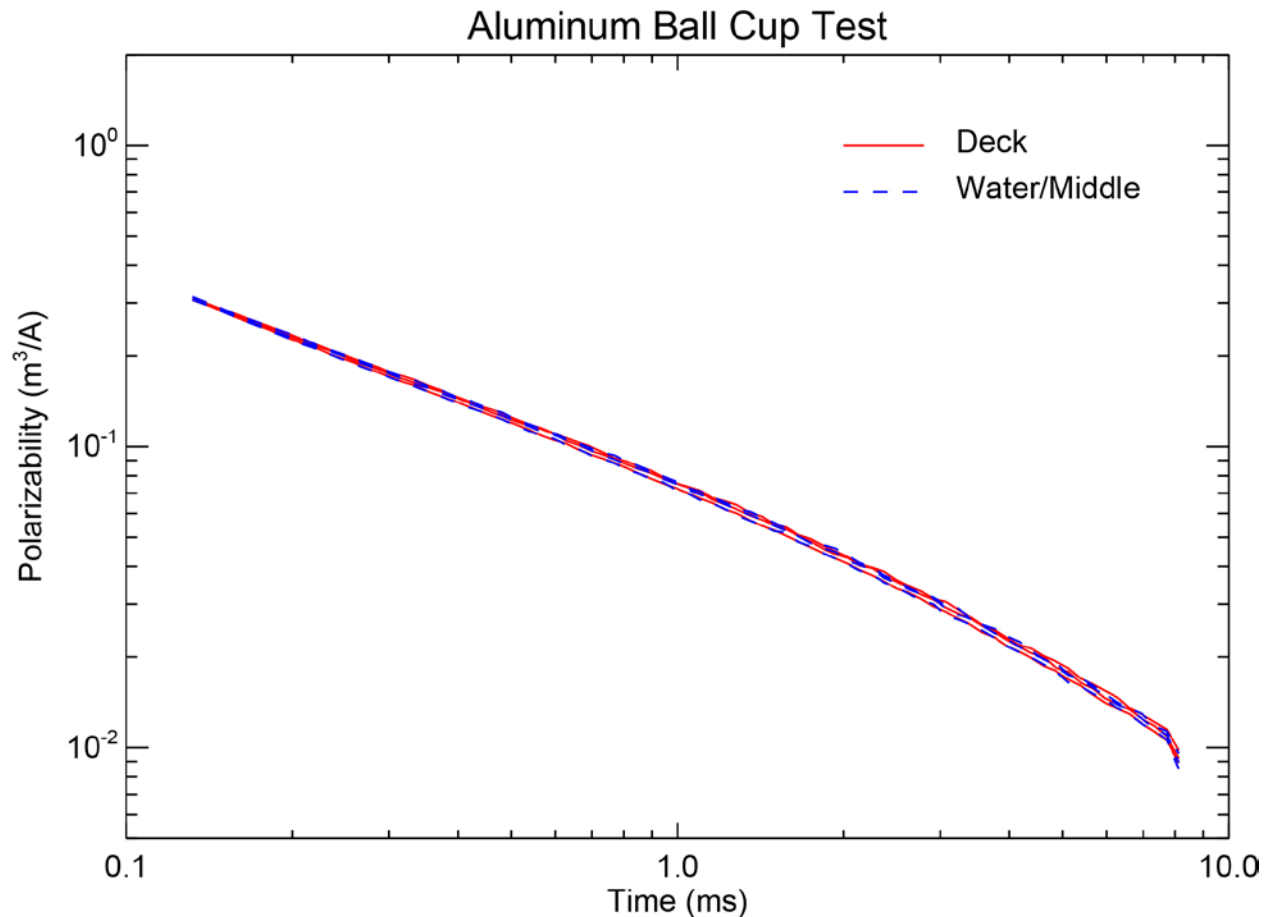
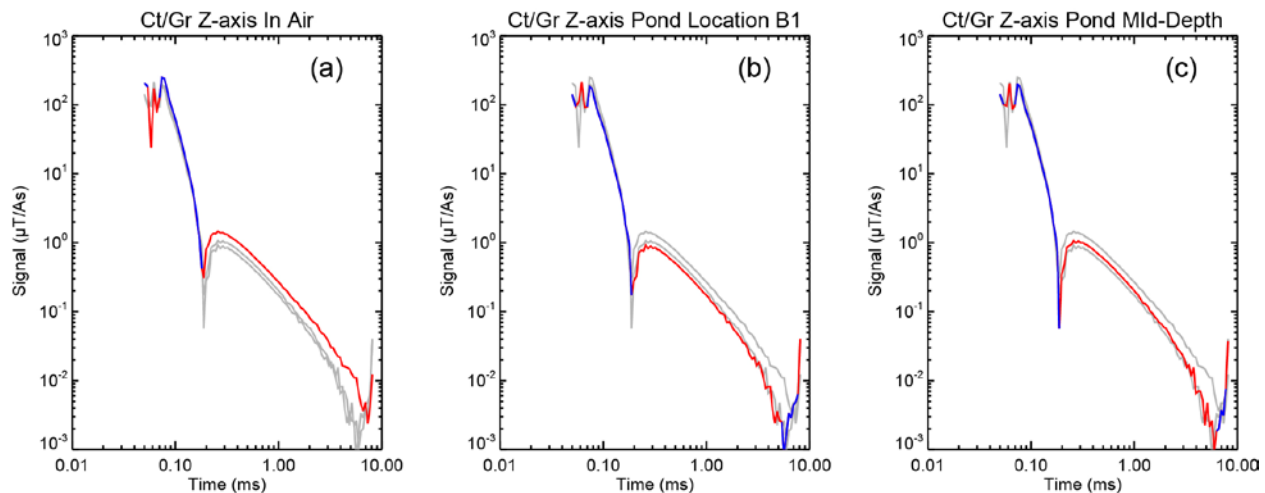


Figure 11. In-air (on deck) and in-water response measurements made with aluminum ball supported above the array on a PVC stand.

## Background Response Test

**Figure 12** shows the average background response for the monostatic TxC/RxG pair (Z-axis) at several locations. In the plot on the left (a) the array is in air on the deck. In the center plot (b) the array is on the bottom of the pond at background location B1 (see **Figure 7**), and on the right (**Figure 12c**) the array is in the pond at mid-depth (approximately 20 ft depth). Negative signals are plotted in red, positive in blue. In each plot the gray curves show the responses at the alternate locations for comparison. The monostatic background Z-axis responses are all similar, and are similar to background responses which have been observed with other TEM systems. Z-axis background responses with the outer loop transmitter (Ht) are similar to the monostatic background responses.



**Figure 12.** Average background response for monostatic TxC/RxG pair, Z-axis, at several locations. (a) Array in air on deck. (b) Array on the bottom of the pond at location B1. (c) Array in the pond at mid-depth. Negative signals in red, positive in blue. In each plot the gray curves show responses at the other locations for comparison.

**Figure 13** compares the background responses for the different receiver axes (Z, Y and X for plots a, b and c respectively) using the monostatic TxC/RxG pair with the array in the pond at background location B1. As before, negative signals are plotted in red, positive in blue. In each plot the gray curves show the responses for the other receiver axes for comparison. Other Tx/Rx combinations (monostatic and bistatic) show similar X- and Y-axis responses. Bistatic Z-axis background responses are qualitatively different from monostatic Z axis responses. They are similar to the monostatic and bistatic X- and Y-axis responses.

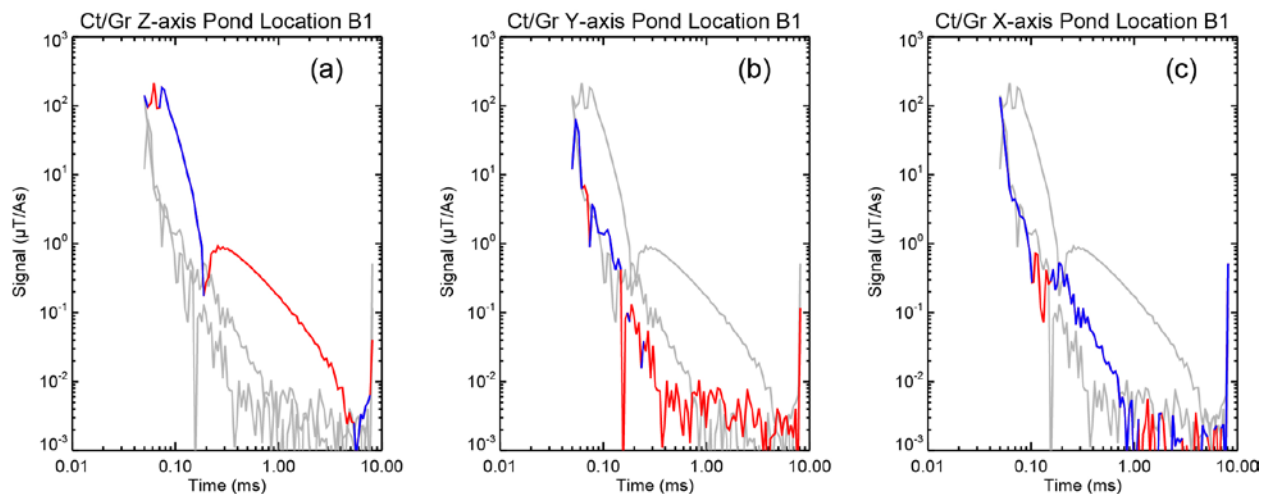


**Figure 13.** Average background response for monostatic TxC/RxG pair at background location B1. (a) Z-axis. (b) Y-axis. (c) X-axis. Negative signals in red, positive in blue. In each plot the gray curves show responses for the other axes for comparison.

Background response variability reflects the basic measurement noise for the array. **Figure 14** shows plots of the measurement-to-measurement background variability for the various transmit receive combinations with the array in the pond on the bottom at background location B1 (solid lines), suspended in the pond at mid depth (dashed lines) and in the air on deck beside the pond (chain dashed lines). The plots are arranged by row with monostatic combinations on the top, bistatic combinations in the middle and receivers paired with the outer transmit loop on the bottom, and by column with receiver Z-axis on the left, Y-axis in the middle and X-axis on the right. For each curve the root-mean-square (RMS) value was calculated for the measurement-to-measurement signal differences vs. decay time for each of the Tx/Rx pairs in the category. The plotted curve is the median of all of the RMS curves in the category (up to seven for monostatic combinations, seventy for bistatic combinations or eleven for outer loop combinations, depending on how many channels were operating properly). In **Figure 14** only measurements taken sequentially with the array stationary were used. The average time difference between measurements was 1½ minutes in all cases. The gray lines show the  $t^{-1/2}$  decay expected for logarithmically gated uncorrelated Gaussian noise:

$$\sigma_G(t) = \sigma_W \sqrt{2\delta t / Nwt}$$

Here  $\sigma_G(t)$  is the gated RMS variability as a function of decay time  $t$ ,  $\sigma_W$  is the sensor white noise level,  $\delta t$  is the sampling interval (0.004 ms),  $N$  is the number of repeats in each measurement (100) and  $w$  is the gate width (5%). The factor of two accounts for differencing the lobes of the bipolar transmit waveform. In all cases beyond about 0.1 ms the gated white noise is apparent. The corresponding sensor white noise levels calculated from the gated noise curves are listed in **Table 2**.

**Table 2. Sensor white noise levels (μT/As) (calculated from curves in Figure 14)**

| Location   | Pond Bottom B1 |       |       | Pond Mid Depth |       |       | Deck  |       |       |
|------------|----------------|-------|-------|----------------|-------|-------|-------|-------|-------|
| Axis       | Z              | Y     | X     | Z              | Y     | X     | Z     | Y     | X     |
| Monostatic | 1.162          | 1.290 | 1.216 | 1.046          | 1.162 | 1.258 | 1.264 | 1.316 | 1.128 |
| Bistatic   | 1.152          | 1.186 | 1.194 | 1.022          | 1.164 | 1.102 | 1.116 | 1.194 | 1.178 |
| Outer Loop | 1.948          | 1.790 | 2.030 | 1.772          | 1.770 | 1.868 | 1.906 | 1.880 | 2.098 |

The average white noise level was 1.18 μT/As with the 40 cm transmit coils and 1.92 μT/As with the large outer loop<sup>6</sup>.

<sup>6</sup> It should be noted that the outer loop noise only differs because the raw receiver signal is normalized by transmit current. The raw receiver noise levels are pretty much equal.



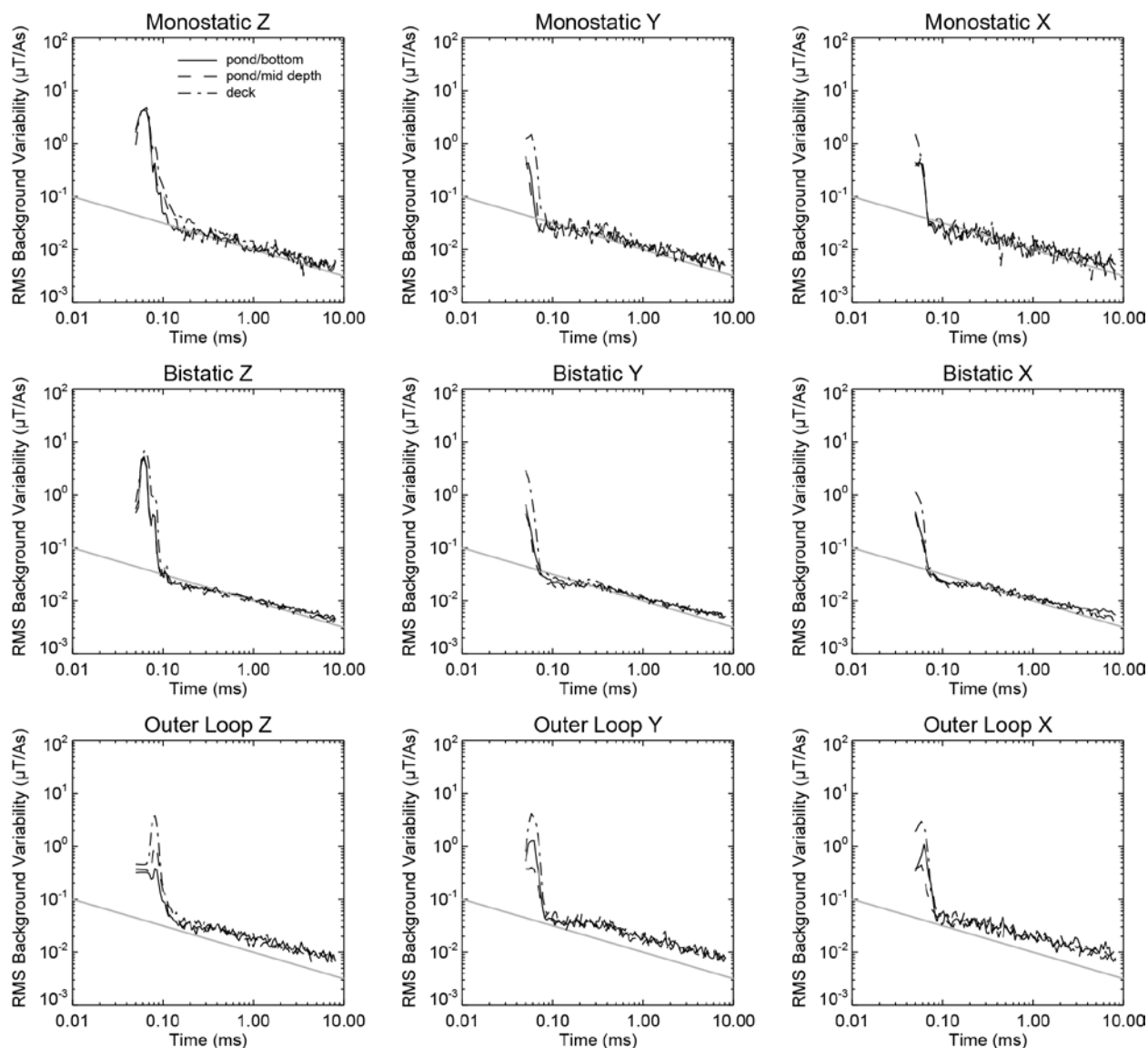


**Figure 14. Median measurement-to-measurement background variability for various transmit/receive combinations. Top row, monostatic Tx/Rx pairs. Middle row, bistatic Tx/Rx pairs. Bottom row outer loop transmitter. Left column Z-axis receive, middle column Y-axis receive, right column X-axis receive. Solid curves are for successive measurements with the array on the bottom of the pond at background location B1. Dashed curves are for successive measurements with the array suspended in the pond at mid depth. Chain-dashed curves are for successive measurements with the array on deck beside the pond. The gray lines show the  $t^{-1/2}$  decay expected for logarithmically gated white noise.**



With longer time intervals and/or changes in the location of the array between measurements additional background variability is observed at early times, as illustrated in **Figure 15**. The layout of this figure is the same as **Figure 14**. Now the solid curves are for measurements as the array was moved from background locations B1 through B4 and back again. The average time interval between measurements was 37.7 minutes. The dashed curves are for measurements taken with the array suspended at mid depth with an average time interval between measurements of 14.9 minutes. A similar effect for successive measurements (average time interval 1½ minutes) is apparent with the array suspended at mid depth and held in position with rope by the divers. The chain dashed curves are for the array on deck with an average time interval between measurements of 18.4 minutes. The gray lines are the same as in **Figure 14**.

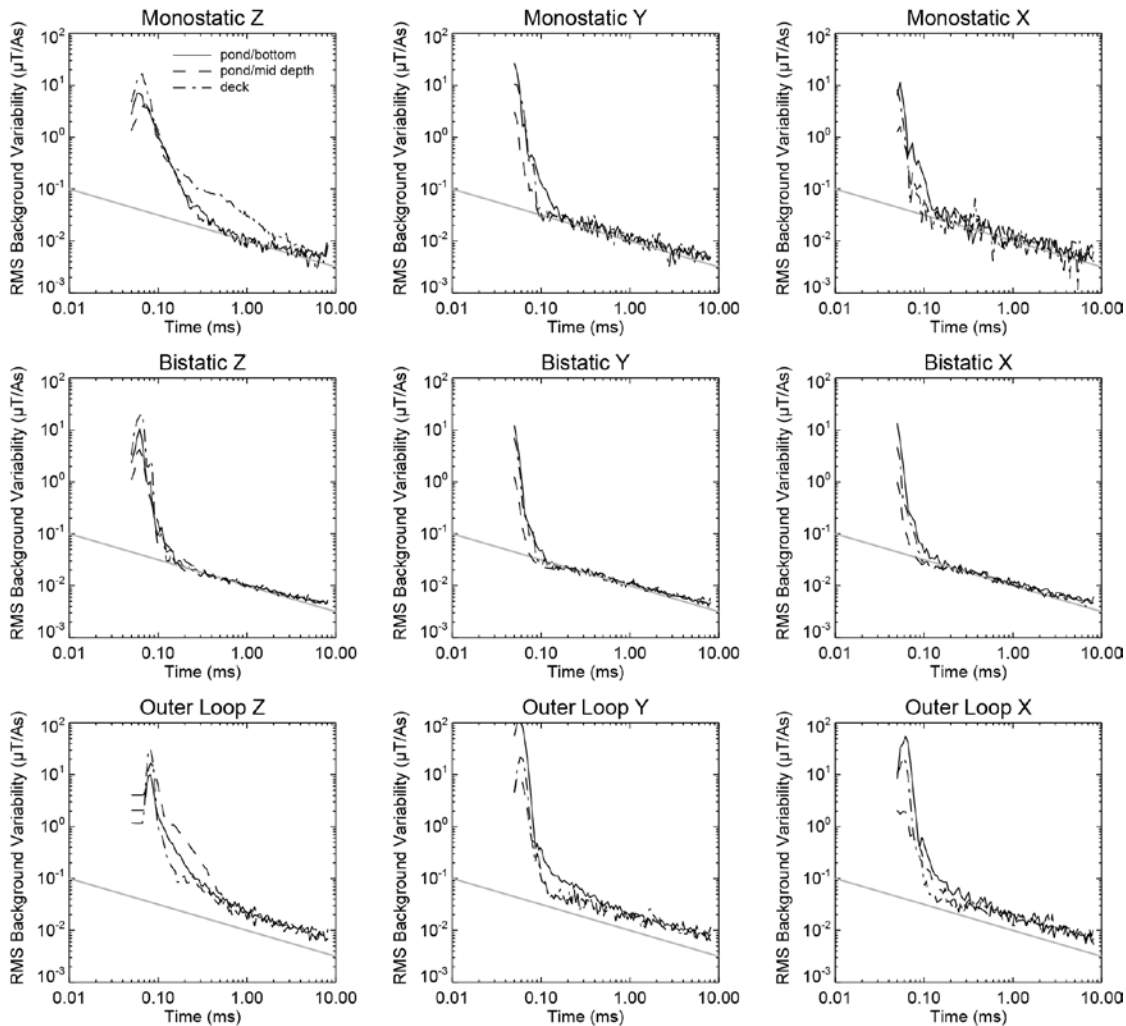


**Figure 15.** Background variability for various transmit/receive combinations for measurements spread out in time and/or space. Top row, monostatic Tx/Rx pairs. Middle row, bistatic Tx/Rx pairs. Bottom row outer loop transmitter. Left column Z-axis receive, middle column Y-axis receive, right column X-axis receive. Solid curves are for measurements with the array on the bottom of the pond at different background locations. Dashed curves are for measurements with the array suspended in the pond at mid depth with an average time between measurements of fifteen minutes. Chain-dashed curves are for measurements with the array on deck beside the pond with an average time between measurements of eighteen minutes. The gray lines show the  $t^{-1/2}$  decay expected for logarithmically gated white noise.

## Board Tests

The board tests were intended to check the accuracy of target locations and polarizabilities determined by inverting array data under controlled conditions. The basic UX-Analyze dipole inversion algorithm was used to fit the data. Malfunctioning data channels were not included and the first 18 time gates ( $t < 0.132$  ms) were not used. The photograph on the left in **Figure 16** shows the test board mounted above the array. The board is a section of 6-inch I-beam with six sets of notches cut into the board for the targets. Medium and large ISO targets are shown resting in the notches. The drawing on the right shows dimensions of the board and its location relative to the array. The top of the test board was nominally 39.3 cm above the center of the array.

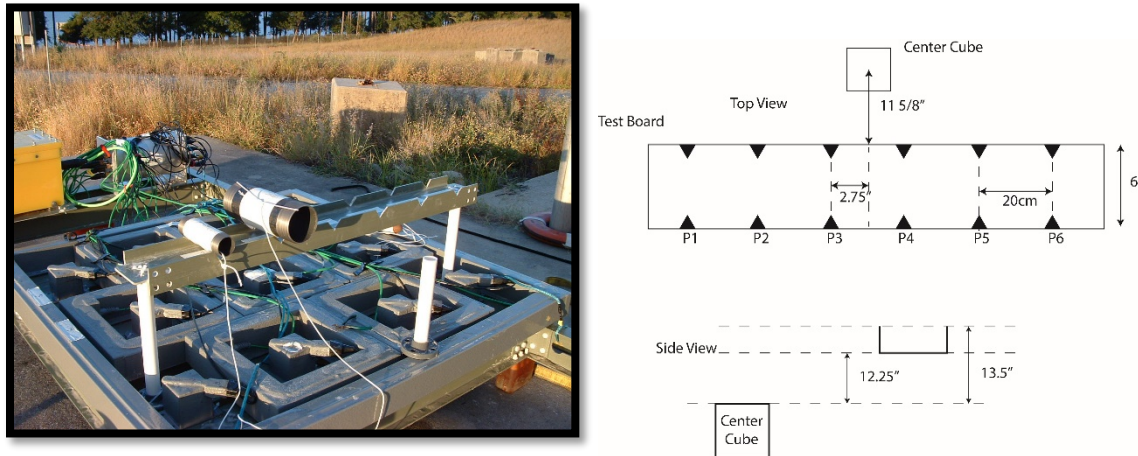


**Figure 16. Left: Test board mounted above array, with medium and large ISO targets. Right: Drawing showing test board dimensions and location relative to array.**

The board test was conducted with the array suspended at mid-depth (approximately 20 ft) in the pond. Three targets were tested: a medium ISO, a large ISO and a solid steel ellipsoid 6 3/8 cm in diameter and 20 cm long. Each target was measured at each of the six notched locations on the board. The basic test procedure was to take a background measurement, measure the target at locations P1 through P3, then take another background followed by target measurements at locations P4 through P6, then a final background.

**Figure 17** shows the board test results for the ellipsoid in the top row, the large ISO in the middle row and the medium ISO in the bottom row. The diagrams on the left compare dipole fit locations ( $\diamond$ ) with nominal target locations (X). The diagrams in the middle compare dipole fit height above the center of the array with nominal target locations. The solid line is the top of the board and the dashed line shows the nominal distance to the center of the target resting on the board. The plots on the right compare calculated polarizabilities (solid curves) with library polarizabilities from ESTCP project MR-201424<sup>7</sup> for the large and medium ISO targets (dashed curves). The ellipsoid is not in the library.

<sup>7</sup> <https://www.serdp-estcp.org/Program-Areas/Munitions-Response/Land/Enabling-Technologies/MR-201424>

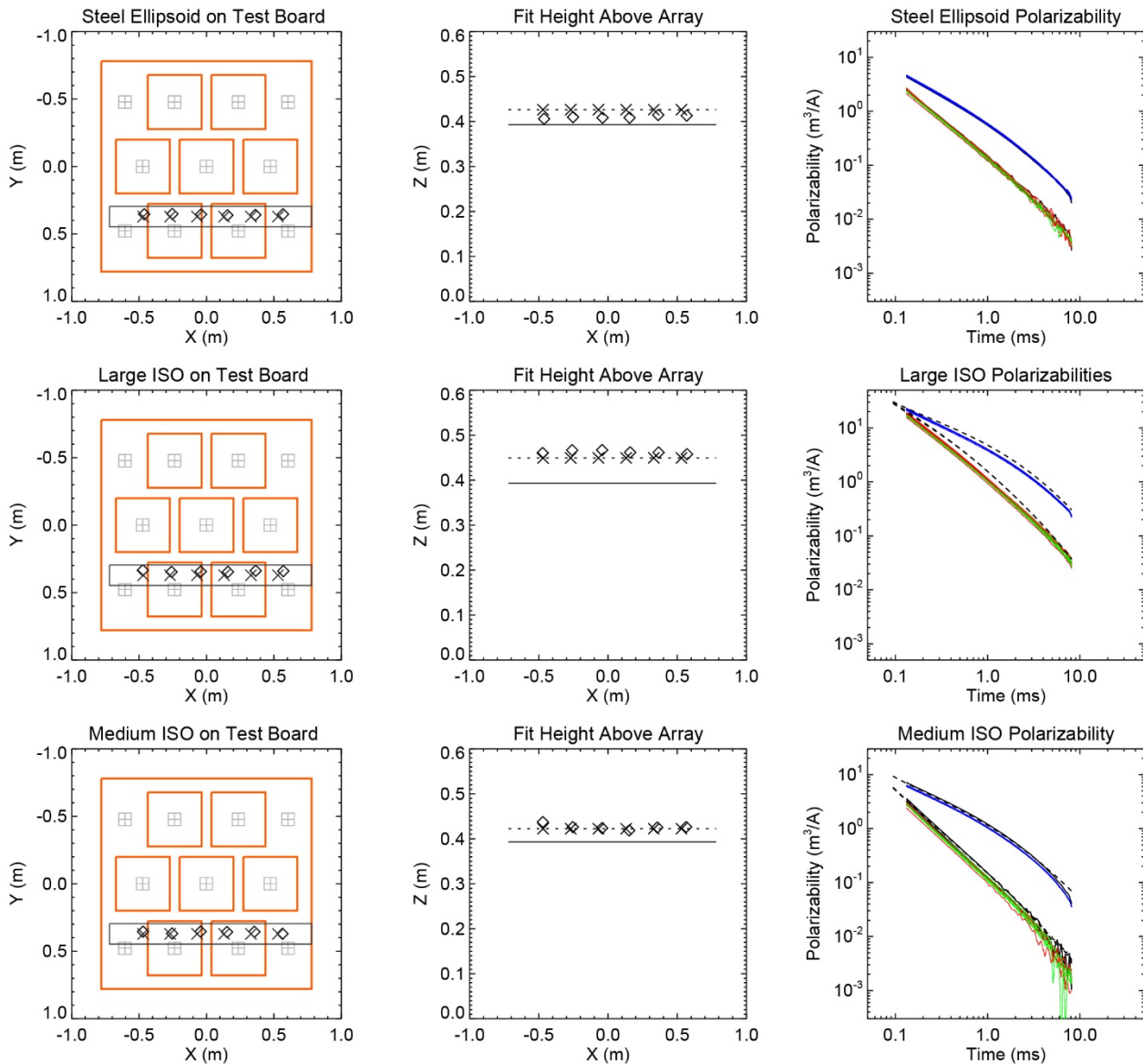


**Figure 17. Board test results for the 6% cm x 20 cm steel ellipsoid (top row), the large ISO (middle row) and the medium ISO (bottom row). The diagrams on the left compare dipole fit locations (O) with nominal target locations (X). The diagrams in the middle compare dipole fit height above the center of the array with nominal target locations. The plots on the right compare calculated polarizabilities (solid curves) with library polarizabilities for the targets (dashed curves). The ellipsoid is not in the library.**

**Table 3** summarizes the results of the board tests. The dipole fit quality as determined by fit coherence (coh = squared correlation between data and dipole fit) was very good. Fit locations were generally within a few cm of the nominal target locations ( $\Delta xy$ ,  $\Delta z$ ). The ellipsoid dipole fit Z-locations are offset down a bit from the nominal Z-locations because the ellipsoid sits lower in the notches on the board than the ISOs. Classification metrics for matching to the library polarizabilities using the UX-Analyze classification algorithm are tabulated in the “library match” column. In all cases the polarizabilities determined by inverting the test board data are good matches to the library polarizabilities.

**Table 3. Dipole fit parameters for targets on test board.**

| pos<br>on<br>board | Steel Ellipsoid     |                    |       |                  | Large ISO           |                    |       |                  | Medium ISO          |                    |       |                  |
|--------------------|---------------------|--------------------|-------|------------------|---------------------|--------------------|-------|------------------|---------------------|--------------------|-------|------------------|
|                    | $\Delta xy$<br>(cm) | $\Delta z$<br>(cm) | coh   | library<br>match | $\Delta xy$<br>(cm) | $\Delta z$<br>(cm) | coh   | library<br>match | $\Delta xy$<br>(cm) | $\Delta z$<br>(cm) | coh   | library<br>match |
| P1                 | 1.9                 | -2.0               | 0.997 | -                | 3.7                 | 1.1                | 0.998 | 0.985            | 1.7                 | 1.5                | 0.993 | 0.979            |
| P2                 | 2.6                 | -1.6               | 0.997 | -                | 2.7                 | 1.7                | 0.998 | 0.981            | 1.5                 | 0.4                | 0.998 | 0.971            |
| P2                 | 3.4                 | -1.8               | 0.996 | -                | 3.9                 | 1.8                | 0.997 | 0.980            | 3.2                 | 0.1                | 0.996 | 0.962            |
| P4                 | 2.7                 | -1.8               | 0.997 | -                | 3.0                 | 1.2                | 0.997 | 0.956            | 2.7                 | -0.4               | 0.998 | 0.932            |
| P5                 | 3.5                 | -1.2               | 0.997 | -                | 4.9                 | 1.2                | 0.998 | 0.981            | 3.0                 | 0.3                | 0.987 | 0.987            |
| P6                 | 4.2                 | -1.3               | 0.997 | -                | 5.1                 | 0.8                | 0.998 | 0.984            | 3.4                 | 0.4                | 0.956 | 0.956            |

## Buried Target Measurements

As described previously, five targets were buried in the sand at the bottom of the pond and their locations are shown by **Figure 7**. Positions O1-O5 are target locations (large ISO, 105mm projectile, 105mm HEAT round, 4-inch x 12-inch aluminum rod, medium ISO) and B1-B4 are background locations where no objects were placed. During the first round of cued target measurements the array had 3-inch feet on it and it was positioned at each target location and moved<sup>8</sup> around over the nominal target locations for six different measurements (see **Table 4**). Background measurements were taken between each of the six-measurement target sequences at each of the five target locations.

For the second series of buried target measurements the 3-inch feet were switched out for 6-inch feet and three measurements (see **Table 4**) were subsequently performed at each target location with the array shifted slightly between measurements. The data were inverted using the UX-Analyze dipole fit algorithm. Malfunctioning data channels were not included, and the first 18 time gates ( $t < 0.132$  ms) were not used. Several of the measurements on the large ISO required two-dipole fits, presumably because there were some metallic objects within the sand bed remaining from other operations conducted in the pond. The calculated polarizabilities were compared with polarizabilities from the ESTCP project MR-201424 library using the UX-Analyze classification algorithm and the results are summarized in **Table 4**. Anomalous early time signal behavior made it impossible to get good fits for the aluminum rod using single or multi-dipole models. This appears to be a problem with background removal rather than anomalous target signal content. Good fits were obtained using only late time ( $t \geq 0.694$  ms) data. Observed signal variation with the aluminum rod relative to the apparent target locations based on late time data is not consistent with signal contributions from anomalous sources such as the electric field (current channeling) effects observed with aluminum targets in salt water in SERDP project MR-2409<sup>9</sup>.

For the most part the measurements produced good fit quality and polarizabilities which were good matches to the library polarizabilities. The true target locations relative to the array are unknown; however, the board tests, discussed in the previous section, indicate an expected match of fit locations to within a few cm of the true target locations. To the extent that the fit locations reflect the actual target location, it appears that most of the time the array was positioned reasonably well over the target. With decent fit quality poor library matches typically occurred for targets outside the array footprint, as illustrated by **Figure 18**. The target locations in which the fit quality was okay but the match to the corresponding library item was less than 0.9, are circled on the figure. One of the medium ISO measurements (O5-6-1) did not converge to an acceptable fit using one or two dipole fit models and the library match failed; visual inspection of the data suggests that the array was not actually over the target and this is a bad

<sup>8</sup> The intent of moving the array between measurements was to compare classification with the object in various locations under the footprint of the array. The initial objective was to perform measurements in various locations within a single quadrant of the array but limited visibility in the pond resulted in a challenging environment within which the divers had difficulty precisely positioning the system.

<sup>9</sup> <https://www.serdp-estcp.org/Program-Areas/Munitions-Response/Underwater-Environments/MR-2409>

measurement. This measurement is represented by the red triangle at the center of the plot. Only two measurements (O1-3-1, O1-3-2) which fit to locations well outside the array footprint (near  $X = -0.4$ ,  $Y = -1.2$ ) had good ( $> 0.9$ ) library matches. They are both measurements on the large ISO taken during the first sequence.



**Figure 18. Buried target fit locations for ISOs and inert munitions. Green locations indicate  $> 0.9$  library match and red indicate  $< 0.9$ . Circled locations indicate where the fit quality was good ( $> 0.5$ ) but the match to the corresponding library item was  $< 0.9$ .**

**Table 4. Cued target fit parameters.**

|                       |                        | Measurement with 3-inch feet |              |              |              |              |              | Measurement with 6-inch feet |        |        |
|-----------------------|------------------------|------------------------------|--------------|--------------|--------------|--------------|--------------|------------------------------|--------|--------|
| Large ISO (O1)        | <i>Measurement ID:</i> | O1-3-1                       | O1-3-2       | O1-3-3       | O1-3-4       | O1-3-5       | O1-3-6       | O1-6-1                       | O1-6-2 | O1-6-3 |
|                       | X (m)                  | -0.37                        | -0.37        | <i>1.12</i>  | <i>1.39</i>  | <i>1.06</i>  | <i>1.10</i>  | -0.38                        | -0.41  | -0.35  |
|                       | Y (m)                  | <i>-1.21</i>                 | <i>-1.20</i> | -0.78        | -0.70        | -0.62        | -0.69        | -0.16                        | 0.11   | 0.43   |
|                       | Z (m)                  | 0.39                         | 0.38         | 0.30         | 0.12         | 0.33         | 0.29         | 0.45                         | 0.44   | 0.41   |
|                       | Fit Coherence          | 0.986                        | 0.996        | 0.997        | 0.991        | 0.999        | 0.997        | 0.998                        | 0.998  | 0.999  |
|                       | Distance (m)           | <i>1.26</i>                  | <i>1.26</i>  | <i>1.36</i>  | <i>1.56</i>  | <i>1.23</i>  | <i>1.30</i>  | 0.42                         | 0.42   | 0.55   |
|                       | Library Match          | 0.919                        | 0.948        | <b>0.861</b> | <b>0.630</b> | <b>0.866</b> | <b>0.816</b> | 0.943                        | 0.948  | 0.908  |
| 105mm Projectile (O2) | <i>Measurement ID:</i> | O2-3-1                       | O2-3-2       | O2-3-3       | O2-3-4       | O2-3-5       | O2-3-6       | O2-6-1                       | O2-6-2 | O2-6-3 |
|                       | X (m)                  | -0.09                        | 0.01         | 0.06         | -0.39        | -0.38        | -0.55        | 0.24                         | 0.21   | 0.18   |
|                       | Y (m)                  | -0.71                        | -0.49        | -0.30        | -0.07        | -0.20        | -0.58        | -0.23                        | 0.00   | 0.35   |
|                       | Z (m)                  | 0.42                         | 0.43         | 0.42         | 0.42         | 0.45         | 0.45         | 0.46                         | 0.43   | 0.45   |
|                       | Fit Coherence          | 0.999                        | 0.996        | 0.989        | 0.993        | 0.991        | 0.998        | 0.992                        | 0.992  | 0.997  |
|                       | Distance (m)           | 0.72                         | 0.49         | 0.31         | 0.39         | 0.43         | 0.79         | 0.33                         | 0.21   | 0.39   |
|                       | Library Match          | 0.957                        | 0.969        | 0.993        | 0.952        | 0.970        | 0.964        | 0.997                        | 0.943  | 0.971  |
| 105mm HEAT (O3)       | <i>Measurement ID:</i> | O3-3-1                       | O3-3-2       | O3-3-3       | O3-3-4       | O3-3-5       | O3-3-6       | O3-6-1                       | O3-6-2 | O3-6-3 |
|                       | X (m)                  | -0.60                        | -0.48        | -0.34        | <i>-0.80</i> | -0.63        | -0.69        | -0.04                        | 0.01   | 0.07   |
|                       | Y (m)                  | 0.27                         | 0.43         | 0.18         | -0.13        | -0.39        | -0.58        | -0.35                        | 0.06   | 0.32   |
|                       | Z (m)                  | 0.41                         | 0.39         | 0.43         | 0.42         | 0.44         | 0.46         | 0.51                         | 0.48   | 0.50   |
|                       | Fit Coherence          | 0.988                        | 0.995        | 0.989        | 0.998        | 0.997        | 0.999        | 0.997                        | 0.996  | 0.994  |
|                       | Distance (m)           | 0.65                         | 0.64         | 0.39         | <i>0.81</i>  | 0.74         | <i>0.90</i>  | 0.35                         | 0.06   | 0.32   |
|                       | Library Match          | 0.929                        | 0.982        | 0.992        | 0.965        | 0.961        | <b>0.697</b> | 0.968                        | 0.986  | 0.981  |
| Aluminum Rod (O4)     | <i>Measurement ID:</i> | O4-3-1                       | O4-3-2       | O4-3-3       | O4-3-4       | O4-3-5       | O4-3-6       | O4-6-1                       | O4-6-2 | O4-6-3 |
|                       | X (m)                  | -0.02                        | 0.08         | 0.29         | -0.36        | -0.53        | -0.45        | 0.11                         | 0.10   | 0.10   |
|                       | Y (m)                  | -0.58                        | -0.30        | 0.16         | 0.08         | 0.17         | -0.34        | <i>-0.83</i>                 | -0.53  | -0.10  |
|                       | Z (m)                  | 0.38                         | 0.42         | 0.47         | 0.49         | 0.52         | 0.42         | 0.38                         | 0.43   | 0.50   |
|                       | Fit Coherence          | 0.997                        | 0.995        | 0.990        | 0.997        | 0.996        | 0.995        | 0.991                        | 0.997  | 0.994  |
|                       | Distance (m)           | 0.58                         | 0.31         | 0.33         | 0.36         | 0.55         | 0.56         | <i>0.83</i>                  | 0.54   | 0.14   |
|                       | Library Match          | -                            | -            | -            | -            | -            | -            | -                            | -      | -      |
| Medium ISO (O5)       | <i>Measurement ID:</i> | O5-3-1                       | O5-3-2       | O5-3-3       | O5-3-4       | O5-3-5       | O5-3-6       | O5-6-1                       | O5-6-2 | O5-6-3 |
|                       | X (m)                  | -0.16                        | -0.13        | 0.00         | -0.42        | -0.34        | -0.14        | ****A                        | 0.41   | 0.42   |
|                       | Y (m)                  | <i>-0.92</i>                 | -0.55        | -0.04        | -0.15        | -0.57        | <i>-0.88</i> | ***                          | -0.20  | 0.50   |
|                       | Z (m)                  | 0.39                         | 0.36         | 0.35         | 0.36         | 0.34         | 0.40         | ***                          | 0.39   | 0.40   |
|                       | Fit Coherence          | 0.990                        | 0.999        | 0.996        | 0.998        | 0.980        | 0.653        | ***                          | 0.988  | 0.992  |
|                       | Distance (m)           | <i>0.94</i>                  | 0.57         | 0.04         | 0.45         | 0.66         | <i>0.89</i>  | ***                          | 0.45   | 0.65   |
|                       | Library Match          | <b>0.714</b>                 | 0.968        | 0.917        | 0.938        | 0.957        | <b>0.273</b> | ***                          | 0.936  | 0.937  |

**Notes:**X, Y and distance values are relative to the center of the array and are *italicized and red* where greater than 0.8m.Library match values below 0.9 are **bold and red**.<sup>A</sup> Did not converge to acceptable fit. Review of the data suggests that this measurement was not collected over the object.

## Performance Objectives

Results with respect to each of the performance objectives identified in the *Underwater Advanced Time-Domain Electromagnetic System Evaluation Plan* (CH2M, 2017) are discussed in the following sections and summarized in **Table 5**.

### **Objective: System is sufficiently waterproofed**

The array remained underwater up to eight hours continuously and no leaks were discovered during field operations or indicated in the data collected.

### **Objective: Calibration method can be used both topside and underwater**

Geometrics did not provide a baseline response plot in advance but a calibration test with an aluminum ball on a PVC pedestal was performed once on deck and once in the water. The pedestal broke after the initial measurements and could not be repeated, however, as shown by **Figure 11**, the results of the test showed an excellent match.

### **Objective: Classification can be achieved if item is anywhere within physical footprint of system**

26 of 28 buried target measurements within the array footprint (initially considered as the entire 1.56 m x 1.56 m area within the outer coil) had a library classification match greater than 0.9. Visual inspection of the data for one of the two failures (medium ISO measurement O5-6-1) suggests that the target was not actually under the array. (An obvious lesson learned from this is that the individual performing the data collection must ensure that a response from a metallic object has been measured prior to moving to the next measurement location.) The remaining measurement that had a library classification match less than 0.9 was measurement O2-3-6 over the 105mm HEAT projectile, which had a match of 0.697. The projectile was within the footprint of the system but, as shown by the circled red square in **Figure 18**, it was at the outer edge (0.90m from the center) near a corner of the array. This result indicates that all objects will not necessarily be successfully classified if located within the footprint of the system if the footprint is considered the entire area within the outer coil. Until a revised footprint is determined, an alternative metric might be the distance of the object from the center of the array. **Figure 19** shows the relationship between the distance from the center of the array of each object (except the aluminum bar) when measured and its library match. Results indicate that all objects within 0.8m of the center of the array when measured were successfully classified (with the exception of medium ISO measurement O5-6-1 discussed earlier in this section.)

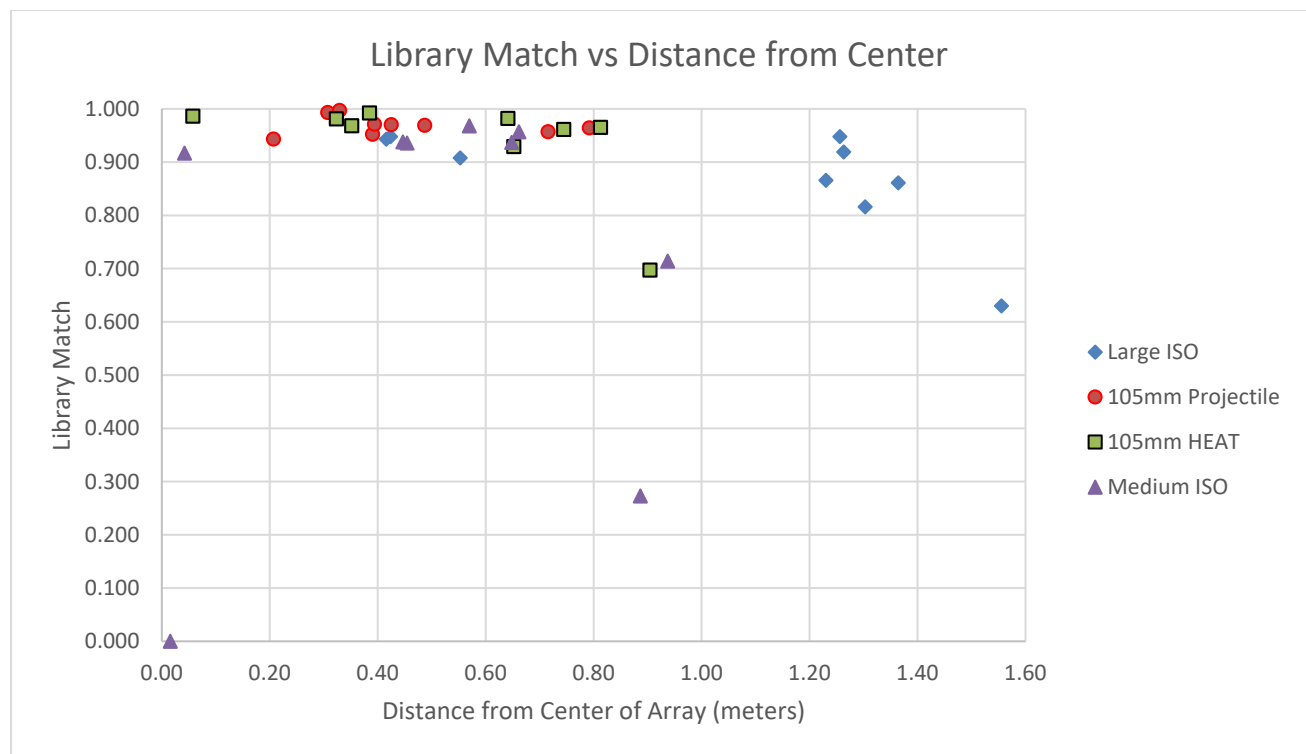


**Figure 19. Graphs showing the relationship of the distance from the center of the array of each object during measurement to the library match.**

### **Objective: Sensor response repeatability (cued surveys)**

The intent of this objective was to record the response from a standard object at the same distance and orientation on a daily basis. As discussed previously, an aluminum ball on a PVC pedestal was to be used for this test but the pedestal broke after the initial day's measurements and was not repeated on the second day. However, multiple measurements over the same object at similar distances from the center of the array show good repeatability in terms of the library match. During the next phase of system evaluation, the sensor response repeatability will be further confirmed.

### **Objective: Sensor can be deployed using winch and donut approach**

The array was easily deployed into the pond using the crane and maneuvered in the water using the inner-tube shallow water lift system (donut) and winch. The divers provided some feedback with respect to modifications, such as handles on the frame, holes in the base of the system for visibility to the bottom, cable management, and improvements to the attachment mechanism for the ropes used to deploy the system with the crane and winch.

Prior to the next deployment the team will attach handles, ensure that the harnesses cannot slip off of the system while being deployed, and a sleeve will be added around all cables to keep them together.

### **Objective: Sensor can be sufficiently maneuvered in underwater environment by divers such that the divers' safety is not compromised**

Feedback from the divers indicated that there were no safety issues related to maneuvering the system underwater.



## Objective: Sensor can be sufficiently maneuvered in underwater environment by divers such that the system can be placed satisfactorily on the desired cue location to collect classification data

The system was easily transported between measurement points in less than 10 minutes; however, as discussed previously, some improvements to the system would make it even easier to transport and effectively position the system over the intended target location. The divers had difficulty ensuring that the target location was under the array footprint in 9 out of the 45 measurements. While 3 of these were within 15 cm of the edge of the array, 6 were between 28 and 60 cm away; all 6 of these were measurements of the large ISO (O1-3-1 through O1-3-6), so clearly there was either an issue with movement of the rope marking the object location or some other factor specific to this set of measurements. (In other words, the inaccuracy may be related to the marking approach used as opposed to the divers' ability to maneuver and place the system.)

A Diver Proximity Test was performed near the end of the field operations to determine whether the procedure employed over the course of the testing of the divers moving 10-20 feet away from the system during measurements was necessary. For this test a measurement was collected at a background location with the divers away from the system and two separate measurements with a diver standing at the edge of the system where the battery and electronics boxes are located. **Figure 20** shows an overlay of the results, which indicates that the presence of the divers had little or no effect and that the time between measurements can be further reduced as the divers do not need to go as far away from the system as they did during the field evaluation.

During the next deployment the team will also employ additional markers and ropes on the sediment surface to assist the divers with appropriate reacquisition of the system for data measurements.

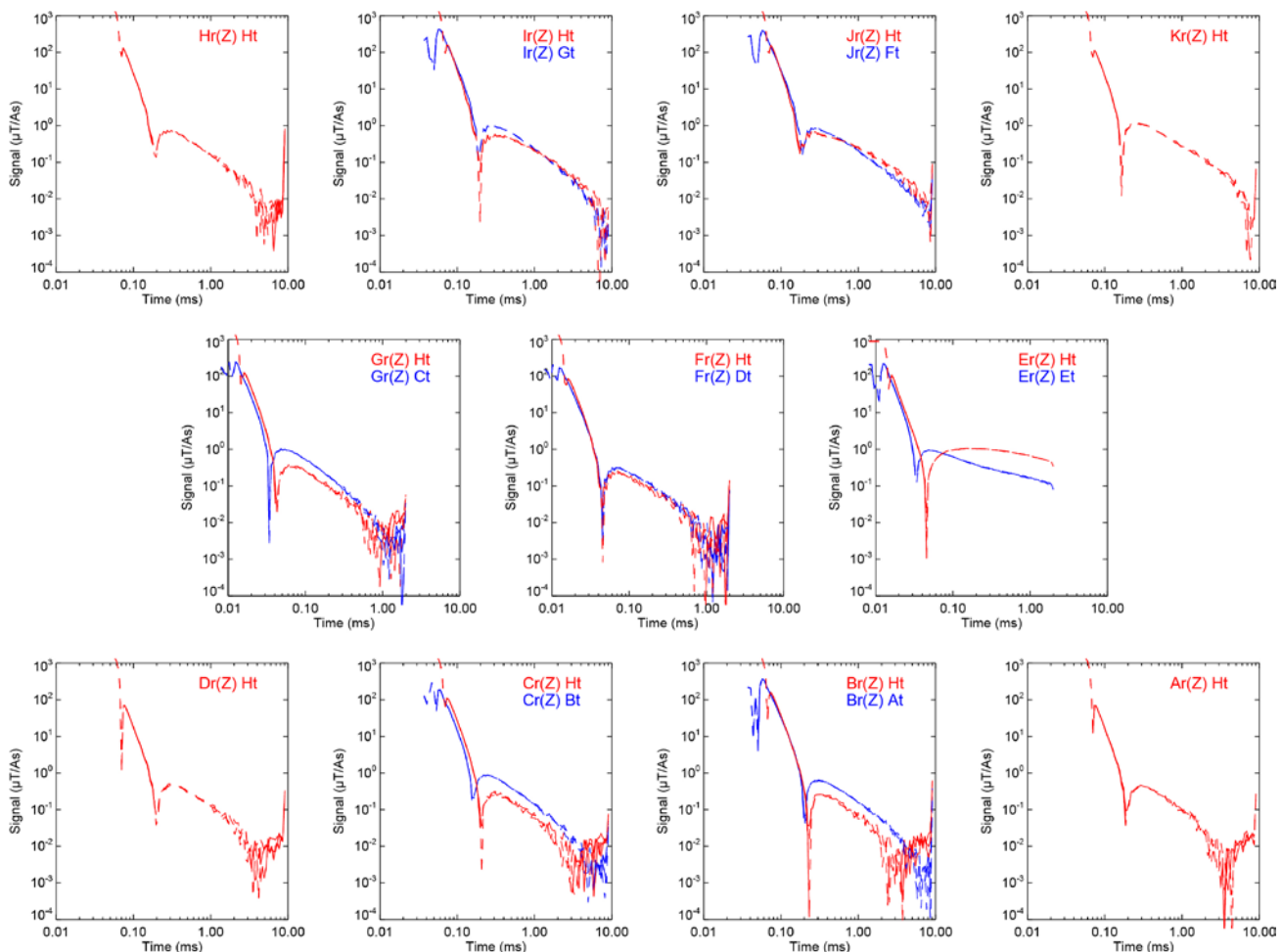


**Figure 20. Overlay of monostatic Z-axis responses (blue) and Z-axis responses with outer (H) transmitter (red) for no diver and two measurements with a diver standing by the battery box. Solid portions are positive signal, dashed portions are when signal is negative.**

### **Objective: Inversion results support classification**

The Fit Coherence was greater than 0.8 for 43 of 45 cued measurements (see **Table 3**). One of the failures, medium ISO measurement O5-3-6, fit to a location 9 cm outside of the array footprint and 0.89 m from the center of the array. For the other failure, medium ISO measurement O5-6-1 discussed in previous sections, the dipole inversion failed and visual inspection of the data suggests that the array was not actually over the target.

### **Objective: Inversion result provides correct position**

Fit locations were generally within a few cm of the nominal target locations for the board tests (see **Figure 9**, **Table 2**), with an average of 3.2 cm and a maximum of 5.1 cm. Exact locations relative to the array were not known for the buried target measurements.

### **Objective: Classification is valid**

28 of 36 buried target measurements had a UX-Analyze classification metric greater than 0.9. All but one of the failures were outside of or near the edge of the array footprint. The other one was medium ISO measurement O5-6-1 (discussed in previous sections) which had a poor fit quality (0.264) and for which the library match failed; visual inspection of the data suggests that the array was not actually over the target.

| Table 5. Performance Objectives and Results  |   |  |  |  |
|--|---|--|--|--|
| Performance Objective  | Metric  | Data Required  | Minimum Acceptable Criteria  | Result   |
| System is sufficiently waterproofed  | No indications that water has leaked into system components   | Data collected by system and visual observation  | Data do not indicate water has entered system components.  | No indications that water leaked into system components  |
| Calibration method can be used both topside and underwater                             | Baseline response plots provided by Geometrics are similar to response in water and on land   | Data collected by system and visual observation  | Response plots of system are reasonably similar to baseline plots – qualitative measurement  | Geometrics did not provide a baseline response plot in advance but a calibration test with an aluminum ball on a PVC pedestal was performed once on deck and once in the water. The pedestal broke after the initial measurements and could not be repeated, however, the results of the test showed an excellent match.   |
| Classification can be achieved if item is anywhere within physical footprint of system | If classification is possible at a location under the physical footprint of the array it is possible at all other locations under the footprint as well | Response curve of metallic object placed at multiple locations under footprint, to include edges | If classification is possible at a single location under the physical footprint of the array it is possible at all other locations under the footprint as well | 26 of 28 buried target measurements within the array footprint had a library classification match > 0.9. Visual inspection of the data for one of the 2 failures (medium ISO measurement O5-6-1) suggests that the target was not actually under the array. The remaining target (105mm HEAT measurement O3-3-6) that had a library classification match <0.9 had a match of 0.697. The projectile was within the footprint of the system but was at the outer edge (0.90m from the center) near a corner of the array. This result indicates that all objects will not necessarily be successfully classified if located within the footprint of the system. All objects within 0.8m of the center of the array when measured were successfully classified (with the exception of the erroneous medium ISO measurement and the aluminum bar.) |
| Sensor response repeatability (cued surveys)   | Standard response to a known target in a known location   | Amplitudes from daily testing over standard item at same distance and orientation                | ≤ 20% Root-Mean-Squared (RMS) variation in amplitude   | An aluminum ball on a PVC pedestal was to be used for this test but the pedestal broke after the initial day's measurements and was not repeated on the second day. However, multiple measurements over the same object at similar distances from the center of the array show good repeatability in terms of the library match.   |

| Table 5. Performance Objectives and Results  |   |  |   |  |
|--|---|--|---|--|
| Performance Objective  | Metric  | Data Required  | Minimum Acceptable Criteria   | Result   |
| Sensor can be deployed using winch and donut approach  | System can be deployed using winch without compromising safety of test personnel, integrity of the system, or property damage | Visual observation of system and deployment components                   | Test personnel are not in danger of being injured and the system or property are not in danger of being damaged   | The array was easily deployed into the pond using the crane and maneuvered in the water using the donut and winch.   |
| Sensor can be sufficiently maneuvered in underwater environment by divers such that the divers' safety is not compromised  | Divers are comfortable that their safety will not be compromised maneuvering the system                                       | Verbal feedback from divers  | Divers indicate they are comfortable that their safety is not compromised   | Feedback from the divers indicated that there were no safety issues related to maneuvering the system underwater.  |
| Sensor can be sufficiently maneuvered in underwater environment by divers such that the system can be placed satisfactorily on the desired cue location to collect classification data | Divers are able to effectively and efficiently maneuver the system to the desired cue location                                | Verbal feedback from divers<br>Time to move system between cue locations | Divers indicate they are able to effectively and efficiently maneuver the system to the desired cue location.<br>Time required to move system between cue locations is less than 10 minutes | The system was easily transported between measurement points in less than 10 minutes; however. The divers had difficulty ensuring that the target location was under the array footprint in 9 out of the 45 measurements. While 3 of these were within 15 cm of the edge of the array, 6 were between 28 and 60 cm away; all 6 of these were measurements of the large ISO (O1-3-1 through O1-3-6), so clearly there was either an issue with movement of the rope marking the object location or some other factor specific to this set of measurements. (In other words, the inaccuracy may be related to the marking approach used as opposed to the divers' ability to maneuver and place the system.) |
| Inversion results support classification   | Modeled response match observed responses   | Fit coherence from inversion   | 0.8 (using UX-Analyze fit coherence calculation)  | The Fit Coherence was greater than 0.8 for 43 of 45 cued measurements. One of the failures, medium ISO measurement O5-3-6, fit to a location 9 cm outside of the array footprint and 0.89 m from the center of the array. For the other failure (medium ISO measurement O5-6-1) the dipole fit did not properly converge and visual inspection of the data suggests that the array was not actually over the target.   |

| Table 5. Performance Objectives and Results |   |  |  |   |
|---|---|--|--|---|
| Performance Objective                       | Metric  | Data Required  | Minimum Acceptable Criteria  | Result  |
| Inversion result provides correct position  | Derived target positions match independent measured positions   | Independent measurement of target in known position and inversion results                  | Offset < 40cm  | Fit locations were generally within a few cm (average of 3.1cm, maximum of 5.1cm) of the nominal target locations for the board tests.  |
| Classification is valid                     | Target polarizabilities for known items match library responses | Dipole inversion parameter values and polarizabilities for known, isolated targets (ISO's) | <25% difference between calculated and library reference polarizabilities<br>UX-Analyze classification metric >0.9 (library match correlation) | 28 of 36 buried target measurements had a classification metric >0.9. All but one of the failures were outside of or near the edge of the array footprint. The other one was medium ISO measurement O5-6-1 for which the dipole fit did not converge properly and for which the library match failed; visual inspection of the data suggests that the array was not actually over the target. |

## Summary and Path Forward

CH2M performed a system evaluation of the Underwater Advanced Time-Domain Electromagnetic System at NSWCPD's freshwater pond facility in October 2016. With minor exceptions, the performance objectives were achieved and the system was demonstrated effective in collecting data used for the classification of munitions in a freshwater environment. The path forward, upon approval by ESTCP, is to prepare for and perform a saltwater evaluation of the full system. The following modifications will be made to the system prior to redeployment:

1. Handles will be attached to make the system more easily maneuverable for the divers
2. The attachment point for the ropes will be modified such that the ropes cannot slip off of the system while being deployed
3. A sleeve will be added around all cables to keep them together